Available online at www.sciencedirect.com

SCIENCE DIRECT

Free Radical Biology & Medicine 38 (2005) 665–677

www.elsevier.com/locate/freeradbiomed

Original Contribution

Downregulation of the human Lon protease impairs mitochondrial structure and function and causes cell death

Daniela A. Bota, Jenny K. Ngo, Kelvin J. A. Davies*

Ethel Percy Andrus Gerontology Center, and Division of Molecular and Computational Biology, 3715 McClintock Avenue, University of Southern California, Los Angeles, CA 90089-0191, USA

Received 9 September 2004; revised 10 November 2004; accepted 11 November 2004
Available online 8 December 2004

Abstract

Lon now emerges as a major regulator of multiple mitochondrial functions in human beings. Lon catalyzes the degradation of oxidatively modified matrix proteins, chaperones the assembly of inner membrane complexes, and participates in the regulation of mitochondrial gene expression and genome integrity. An early result of *Lon* downregulation in WI-38 VA-13 human lung fibroblasts is massive caspase 3 activation and extensive (although not universal) apoptotic death. At a later stage, the surviving cells fail to divide, display highly abnormal mitochondrial function and morphology, and rely almost exclusively on anaerobic metabolism. In a selected subpopulation of cells, the mitochondrial mass decreases probably as a result of mitochondrial inability to divide. At this final point the *Lon*-deficient cells are not engaged anymore in apoptosis, and are lost by necrosis or "mitoptosis." Our results indicate that mitochondrial Lon is required for normal survival and proliferation; a clear impetus for Lon's evolutionary conservation.

Introduction

Lon is the best evolutionarily conserved ATP-stimulated protease [1], with homologues identified in a number of bacterial species such as *Escherichia coli* [2], *Bacillus brevis* [3], and *Myxococcus xantus* [4,5]; the yeast *Saccharomyces cerevisiae* [6]; and the mitochondria of mammals [7–9]. This high level of conservation suggests that Lon might play a very important role in the maintenance of mitochondrial homeostasis, and in the bioenergetics and survival of cells.

In *E. coli*, the Lon gene product, protease La, is involved in the degradation of abnormal polypeptides [10,11], and a number of short-lived proteins with important regulatory functions. These include the SOS response proteins, UmuD and UmuC [12], the DNA damage-induced SulA which acts as a cell division inhibitor after ultraviolet light damage [13], and RcsA which is involved in capsular polysaccharide synthesis [14]. Lon-deficient *E. coli* cells display a number of unusual phenotypic features, such as filamentous growth [15], mucoid colony formation [14], and an extended growth lag when shifted from a rich to a minimal medium, because of their inability to degrade free ribosomal proteins and generate amino acids required for the synthesis of key adaptative enzymes [16].

The yeast homologue PIM 1 performs essential functions in yeast mitochondria. Δ*pim1* mutants are respiratory deficient, are unable to utilize nonfermentable substrates as their sole carbon source [6,17], and have impaired ability to degrade mitochondrial matrix proteins which tend to accumulate as electron-dense inclusions [17]. In addition, these strains are unable to maintain functional mitochondrial (mt) DNA [18,19]. Stabilization of mtDNA in *Δpim1* mutants depends on protein degradation, and has been achieved only by expressing a proteolytically active Lon variant [20]. PIM1 involvement in DNA maintenance might be explained by the fact that the human homolog of PIM1 is able to bind to mitochondrial promoters, and may control mitochondrial DNA replication and gene expression by

Abbreviations: mt, mitochondrial; EMEM, Eagle's minimum essential medium; EPEI, ethoxylated polyethylenimine; PI, propidium iodide; BrdU, bromodeoxyuridine; TMB, tetra-methylbenzidine; FBS, fetal bovine serum.

* Corresponding author. Fax: (213) 740 6462.
E-mail address: kelvin@usc.edu (K.J.A. Davies).

0891-5849/$ - see front matter © 2004 Elsevier Inc. All rights reserved.
doi:10.1016/j.freeradbiomed.2004.11.017

degrading regulatory proteins involved in repressing replication [21], or modulating the accumulation/activation of regulatory proteins involved in preserving the integrity of the mitochondrial genome [22]. The chaperone function of PIM1 is independent of its proteolytic function. Therefore, overexpression of even a proteolytically inactive PIM1 can rescue the defects in respiration-dependent growth and inner membrane complex assembly generated by inactivation of the Afg3p and Rca1p AAA metalloproteases [23].

The functions of the mammalian Lon protease are less well described, although aconitase [24] and the SP-22 mitochondrial protein [25] have been identified as substrates. Mammalian Lon can also act as a chaperone, independent of its proteolytic activity, and it promotes the assembly of cytochrome *c* oxidase (COX) subunits. Recently published data [26] show that in vitro the human Lon protease binds GT-rich DNA sequences overlapping the light-strand promoter of human mtDNA as well as GT-rich sequences on the heavy strand of mtDNA and GU-rich RNA. Lon protease also interacts wit mtDNA polymerase γ and the twinkle helicase, in a yet unknown mechanism [26]. Lon expression occurs at different levels in all human tissues so far studied [27,28], and is modulated by aging [29]. Enhanced mitochondrial biogenesis is associated with increased expression of the Lon protease [30], and both endoplasmic reticulum stress and hypoxia seem to be able to induce its production [31].

We have previously reported that *Lon* downregulation, by antisense oligomorpholine treatment of WI-38 VA-13 human lung fibroblasts, leads to impaired mitochondrial proteolysis and accumulation of both native and oxidized aconitase [24]. We next reasoned that an antisense oligomorpholine approach to study *Lon* functions, by gradually increasing Lon deficiency (recognizing that a *Lon* deletion mutant would be lethal), actually provides an excellent opportunity to test whether the multiple roles proposed for *Lon* in bacteria and lower eukaryotes are relevant to human beings. Therefore, we now report how the various cellular roles that Lon plays are sequentially affected by *Lon* downregulation, and how loss of Lon functions compromises the performance and survival of human cells.

Experimental procedures

Materials

All chemicals and reagents were obtained from Sigma unless otherwise specified.

Cell culture and cell survival/proliferation analysis

Human WI-38 VA-13 lung fibroblasts (ATCC) were grown in Eagle's minimum essential medium (EMEM) supplemented with 10% fetal bovine serum, penicillin (100 units/ml), and streptomycin (100 μg/ml). The cultures were grown under an atmosphere of 19.9% oxygen and 5% CO_2 in a humidified 5% CO_2 incubator, at 37°C. Cells were subcultivated at confluency. The medium was changed every other day before the oligonucleotide treatment and every day after the oligonucleotide treatment.

For the analysis of cell survival/proliferation, live, attached cells were harvested by trypsinization at various time points and counted in a Z1S Coulter Particle counter (Coulter). Pictures of cells were also taken, at various times, using a Nikon Phase Contrast 2 microscope at 10× magnification.

Oligonucleotides and delivery

We used a custom (Gene Tools, LLC) antisense morpholino oligonucleotide directed against the *lon* gene to downregulate *lon* in WI-38 VA-13 cells. This oligonucleotide (CGTAGCCAGTGCTCGCCGCCATAGC) is complementary to bases 31 to 55 of *lon* exon 1. A standard control sequence (CCTCTTACCTCAGTTACAATTTATA) that has no target and no significant biological activity (Gene Tools, http://www.gene-tools.com) was also tested. Delivery was achieved by using a weakly basic delivery reagent, ethoxylated polyethylenimine (EPEI). The cells were incubated in the presence of the delivery system for a total of 3 h, as suggested by the manufacturer. Final oligonucleotide concentration in the delivery medium was 1 μM. The delivery medium was then removed, and the cells were grown in fresh EMEM medium and harvested at the time points described. The antisense morpholino oligonucleotide system we used has high and predictable activity inside the cell and is immune to nucleases, which allowed us to use a single treatment [32]. Because of our previous experience with this system [24], we were able to downregulate *lon* very efficiently. Four days after treatment, we were no longer able to detect Lon protein by Western blot analysis, and the mitochondrial ATP-stimulated proteolytic activity was 87% lower in the *lon* antisense oligonucleotide-treated cells then in the control oligonucleotide-treated cells.

Apoptosis analysis by flow cytometry

Adherent WI-38 VA-13 cells (10^6 per experiment) were collected and fixed in 70% ethanol for 2 h. After fixation, the cells were pelleted and suspended in 1 ml propidium iodide (PI)/ Triton X staining solution containing 0.1% Triton X-100, 20 μg/ml PI, and 200 μg DNase-free RnaseA and incubated for 30 min at room temperature. At the end of the incubation time, the cells were subjected to fluorescence-activated cell-sorting analysis of DNA content. The percentage of cells with subdiploid DNA content was taken as a measure of the apoptotic rate of the cell population.

Z-VAD-FMK treatment and caspase-3 assay

WI-38 VA-13 human lung fibroblast cells treated with *lon* antisense oligonucleotide or the matched control oligonu-

cleotide were grown in 25 cm^2 flasks. Z-Val-Ala-Asp(Ome)-FMK (Z-VAD-FMK), a caspase-3 inhibitor from Enzyme Systems Products (Livermore, CA) was added to a final concentration of 50 μM to the cell media after oligonucleotide treatment. The cell media contained 2 μl of DMSO/ 1 ml of EMEM, either as Z-VAD-FMK solvent or as a vehicle control.

Caspase-3 activity was measured in cell extracts, using CPP32/caspase-3 colorimetric protease assay kit from MBL. WI-38 VA-13 human lung fibroblast cells (10^6) were harvested 2, 4, 6, and 8 days after the treatment with oligonucleotides, pelleted at 1500 rpm for 10 min, and resuspended in cell lysis buffer (on ice). The supernatant was separated from the pellet by centrifugation at 10,000*g*. Two hundred micrograms of protein cell extract (supernatant) was incubated with reaction buffer and 200 μM DEVD-pNA substrate at 37°C for 1 h. Protein concentration was determined using the BCA assay (Pierce) or the DC assay (Bio-Rad). Spectrophotometric detection of the EVD-pNA cleavage product, pNA, was performed at 400 nm in a 96-well plate, using a Spectra Max 250 Plate Reader (Molecular Devices). Background readings from cell lysates and buffers were subtracted from the sample values. The results were expressed as percentage of readings from cell lysates of samples grown in the presence of DMSO, but not subjected to the oligonucleotide treatment.

Bromodeoxyuridine (BrdU) incorporation

We measured BrdU incorporation in adherent cells using the BrdU cell proliferation assay from Oncogene. WI-38 VA-13 human lung fibroblast cells treated with *Lon* antisense oligonucleotide, or the matched control oligonucleotide were seeded 6 h before each experimental point at a density of 10^4 cells per well in 96 well culture dishes. We incubated the cells with BrdU for 2 h, and then the cells were fixed and permeabilized. Monoclonal anti-BrdU antibody was added to each well for 1 h, after which the unbound antibody was washed away, and horseradish peroxidase-conjugated secondary antibody was added. Conversion of the chromogenic substrate tetra-methylbenzidine (TMB) was measured after 15 min of incubation in the dark, at dual wavelengths of 450–540 nm, using a Spectra Max 250 plate reader (Molecular Devices).

Uridine treatment

Uridine (Sigma) was prepared [33] as a 10 mg/ml stock solution in distilled water, filter sterilized, and stored at −20°C. WI-38 VA-13 cells were grown after the oligomorpholine treatment in the absence or presence of uridine (100 μg/ml). At various time points, cells from individual plates were trypsinized and counted.

Respiration measurements

WI-38 VA-13 cells (10^7) were trypsinized, suspended in 10 ml of complete culture media, and counted. After centrifugation (1000*g*, 5 min), 5×10^6 cells from each experimental group were suspended either in 1.5 ml of air-saturated complete culture medium (for measurements on intact cells) or in 1 ml of medium A (20 mM Hepes, pH 7.1, 250 mM sucrose, and 10 mM $MgCl_2$), for measurements on permeabilized cells, as previously described [33]. Permeabilization was achieved by adding digitonin to 100 μg/5×10^6 cells; a concentration that permeabilizes the plasma membrane, but leaves the mitochondrial membranes intact [34]. After addition of digitonin, the cells were washed, collected by centrifugation (350*g* for 3 min), and resuspended in air-saturated respiration medium (medium A, plus 1 mM ADP and 2 mM potassium phosphate). Oxygen consumption for intact and permeabilized cells was measured with a Clark-type oxygen electrode in a magnetically stirred, water-jacketed cell, at 37°C (Digital Model 10, Rank Brothers, LTD), calibrated over 0–100% scale. The initial oxygen concentration under these conditions was taken to be 217 nmol/ml.

For the permeabilized cells, oxygen electrode recordings were continued after successively adding the following substrates and inhibitors: glutamate (5 mM) and malate (5 mM) for complex 1 activity measurement; 0.1 μM rotenone (complex 1 inhibitor) and succinate (5 mM) for complex 2 activity determination; 10 mM malonate (complex 2 inhibitor) and α-glycerophosphate (5 mM) for complex 3 activity; 20 μM antimycin (complex 3 inhibitor) plus ascorbate (10 mM) and TMPD (200 μM) as complex 4 substrates; and, finally, 0.1 mM KCN to inhibit complex 4 activity [35,36]. These compounds were added with individual Hamilton syringes from 100 to 200 times concentrated frozen or fresh stock solutions.

Transmembrane potential determination

Mitochondrial transmembrane potential was assessed using the MitoLight ($C_{25}H_{27}Cl_3N_4$) Mitochondrial Indicator from Chemicon International, Inc. Adherent cells, 4 days after oligonucleotide treatment, were grown in 12.5 cm^2 plates and incubated with MitoLight for 1 h. The cells were observed by fluorescence microscopy, and pictures were taken in different fields. Green (527–530 nm) and red (585–590 nm) channel fluorescence was quantified by densitometry (IP Lab) and expressed in arbitrary units.

Mitochondrial mass estimation by FACS analysis

WI-38 VA-13 human lung fibroblast cells were treated with antisense *lon* morpholino oligonucleotide, or the

matched control oligonucleotide. Four or 6 days after treatment, the cells (5×10^5) were trypsinized and incubated with Mito Fluor Red 589 (Molecular Probes) for 45 min. Mito Fluor Red 589 accumulates in mitochondrial membrane lipids (regardless of membrane potential). FACS analysis was performed at 588 nm (emission) and 622 nm (excitation), as recommended by the manufacturer.

Electron microscopy analysis

WI-38 VA-13 human lung fibroblasts were harvested 4 days after the oligonucleotide treatment. We followed a similar protocol to that used for visualization of mitochondrial defects produced by *lon/pim1* downregulation in *S. cerevisiae* [17]. The cells were prepared by fixation in potassium permanganate, infiltrated with Spurr's resin, sectioned, and contrasted with Reynold's lead citrate. Pictures of mitochondrial defects were taken in many different sections, at 10,000 and 20,000× magnification, and the phenotypes described were equally widespread in all the fields studied.

Results

Lon-depleted cell phenotype is characterized by increased cell death and inability to grow

We treated WI-38 VI-13 human lung fibroblasts with morpholino oligonucleotides directed against the *lon* protease sequence, or with a control oligonucleotide, and we obtained a significant downregulation of Lon in the antisense oligonucleotide-treated cells. Four days later, we were not able to detect Lon expression by Western blot in the Lon-deficient cells (Fig. 1A), and the ATP-stimulated proteolytic activity was 87% less in the cells treated with the antisense *lon* oligonucleotide than in control cells, as previously reported [24].

It is worth noting that our oligonucleotide delivery protocol contains two potential causes for cell stress: the ethoxylated polyethylenimine delivery reagent, and the 3 h of serum deprivation required during the delivery stage. Polyethylenimine/DNA complexes have been shown to induce cellular stress and concentration-dependent cell death at up to 9 h after delivery [37], but no

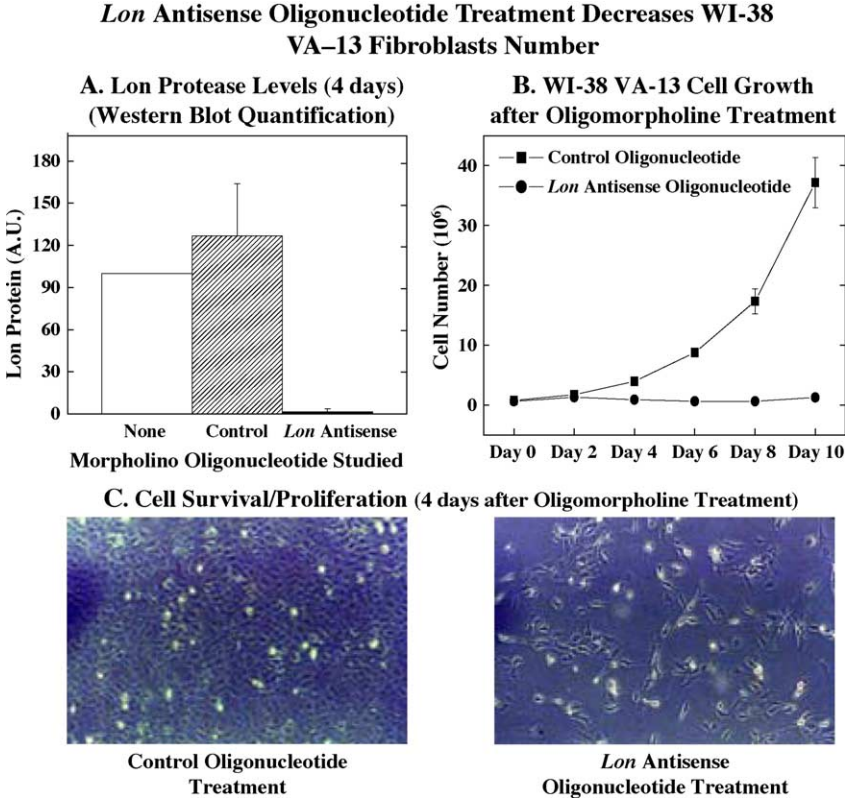

Fig. 1. The impact of Lon protease downregulation on WI-38 VA-13 human fibroblasts. WI-38 VA-13 cells treated with *lon* antisense oligonucleotide, or the matched control oligonucleotide, were grown in EMEM media supplemented with 10% FBS. Multiple 12.5 cm^2 flasks were seeded with 10^6 cells 6 h before the start of the experiment, and the cells were subcultured every other day. (A) Summary of total Lon protease levels (arbitrary units) from three different experiments in which Lon was visualized by Western blotting and quantified by densitometry (IP lab). The measurements were performed 4 days after the oligonucleotide treatment and results are means ± standard errors. (B) At the time points indicated, cells from individual plates were trypsinized and counted. (C) Pictures of the cells were taken 4 days after treatment under an inverted microscope. Representative pictures are shown.

long-term effects. Serum deprivation is a known inducer of apoptosis in various cell lines [38–40], and for fibroblasts apoptosis becomes significant only after at least 24 h [40]. However, even more sensitive cells, such as neuronal precursors, fully recover their viability [38] when serum-deprived for up to 4 h and then grown in complete medium. Under our experimental conditions, no significant cell death/detachment was observed in the cells treated with the control oligonucleotide/EPEI complex, and the same doubling time of 2 days (similar to the doubling time of WI-38 VI-13 fibroblasts grown in regular media without any treatment) was observed in cells treated with the control oligonucleotide for the entire 10-day period studied.

When we counted the number of live, attached cells in the cell flasks treated with the antisense *lon* oligonucleotide/EPEI complex, consistently less cells were found than in the control oligonucleotide-treated cells, despite the fact that both cultures started with a similar number of cells (Fig. 1B). Two days after the treatment, cells treated with control oligonucleotide had more than doubled their number, from 0.78×10^6 to 1.73×10^6, a 120% increase. In contrast with these control results, cells treated with the *lon* antisense oligonucleotide only increased their cell number by 60% during the first 2 days after treatment.

After 2 days, the number of cells in the colonies treated with *lon* antisense oligonucleotide actually began to decline, from 1.3×10^6 cells counted 2 days after treatment to 0.9×10^6 cells on the fourth day of the experiment; a cell number four times lower than that of the control cells. The number of *lon* antisense oligonucleotide-treated cells continued to decrease by a similar percentage (30%) between Day 4 (0.9×10^6) and Day 6 (0.64×10^6), and then remained stagnant for the next 2 days.

An increased number of dead, detached cells were observed floating in the culture media of the Lon-deficient cells. When pictures of the cell plates were taken (Day 4), two characteristics were observed: (1) the antisense *lon*-treated cells were less numerous, and (2) a significant percentage of the cells still present on the plates were partially detached (Fig. 1C).

Lon downregulation induces early apoptotic cell death in WI-38 VA-13 fibroblasts by a mechanism involving caspase-3

To examine the cause of cell death in the WI-38 VA-13 fibroblasts we used flow cytometric analysis of the DNA content (Fig. 2A). Reduced fluorescence of propidium iodine-stained DNA has been described in apoptotic cells, initially as a consequence of chromatin condensation to a state of reduced accessibility [41] and, at a later stage, because of partial loss of DNA content due to activation of endogenous endonuclease and diffusion of the low molecular weight fragments from the cells [42]. It has also been shown that necrosis does not result in generation of a DNA subdiploid peak [43,44]. Four days after treatment, the percentage of adherent *lon* antisense oligonucleotide-treated cells having a subdiploid DNA content was 6.8%, sixfold more than the percentage of subdiploid cells in the control group (1.1%). This number actually underestimates apoptosis because it includes only the apoptotic cells that were still attached to the plates, and not the cells that were already detached and floating in the media. The number of cells that actually died by apoptosis could be calculated as the difference between the predicted cell number (from controls) and the actual cell number, divided by the growth rate estimated by bromodeoxyuridine incorporation. Using this approach it appears that apoptotic cell death was actually closer to 26% between Days 0 and 2, and 69% between Days 2 and 4 of antisense treatment (see Discussion for more details).

Since caspase-3 is a key enzyme involved in the early stages of apoptosis [45,46], we next analyzed cell survival and caspase-3 activity in cells treated with *lon* antisense or control oligonucleotides, and grown in the presence or absence of the caspase-3 inhibitor, Z-VAD-FMK (Figs. 2B and C). As previously described [24], after treatment with *lon* antisense oligonucleotides, Lon protease expression and activity declined and cell number began to decrease (Fig. 2B). Cell death was an important cause of this decline in overall cell number. In contrast, cells treated with the control oligonucleotide grew normally, and cell numbers increased from 3.75×10^6 to 9.68×10^6 between Days 0 and 6.

Between Day 0 and Day 4, the survival of *lon* antisense oligonucleotide-treated cells was improved by Z-VAD-FMK treatment, and the cell number in this group increased 100% by Day 2, and 40% between Day 2 and Day 4. Z-VAD-FMK was less effective in increasing the cell number after Day 4 (41% increase between Days 4 and 6, and 14% increase between Days 6 and 8), suggesting that a second, different mechanism might be also involved in slow growth at the later stages of Lon deprivation (Fig. 2B).

When using oligonucleotides it is important to determine if the delivery protocol itself is toxic or even apoptotic. No significant cell death was seen in the control oligonucleotide-treated cells; however, even though, on the second day after treatment, the level of caspase-3 activity was almost double the baseline caspase-3 activity in nontreated cells (Fig. 2C). In accord with this observation, although Z-VAD-FMK addition effectively decreased the caspase-3 activity in these cells (Fig. 2C), it failed to cause any significant increase in cell number in the control group (Fig. 2B), suggesting that apoptosis was not a significant problem. Four days after transfection, the control oligonucleotide-treated cells had reduced their caspase-3 activity to baseline levels. This apparent paradox at low levels of caspase-3 activation has been seen before [47], and is probably explained by the cells ability to recover from a partial caspase-3 (potentially pro-apoptotic) stimulus, without necessarily entering apoptosis.

In contrast, the antisense *lon* oligonucleotide-treated cells had a much higher activation of caspase-3: 2 days after the start of the experiment, caspase-3 activity was 600% higher than baseline levels, and declined more slowly (still 230%

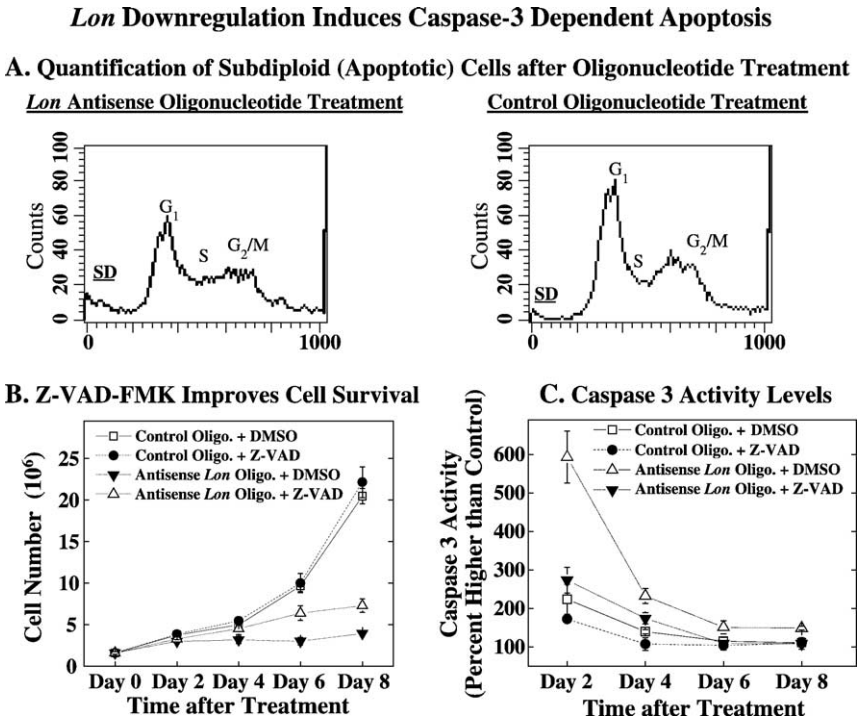

Fig. 2. Lon protease deficiency causes early apoptotic cell death by a caspase-3-dependent mechanism. (A) WI-38 VA-13 cells treated with *lon* antisense oligonucleotides display subdiploid (SD) DNA content. *Lon* antisense and control oligonucleotide-treated cells were harvested 4 days after treatment, and subjected to propidium iodine staining and flow cytometric analysis of DNA content. The total number of cells analysed for each experiment was 15,000. (B) Z-VAD-FMK improves cell survival. WI-38 VA-13 human lung fibroblasts treated with *lon* antisense oligonucleotide or the matched control oligonucleotide were grown in 25 cm^2 flasks. Z-VAD-FMK was added to a final concentration of 50 μM to the cell media, which always contained 2 μl of DMSO/1 ml of EMEM, either as Z-VAD-FMK solvent or as the vehicle control. At the time points indicated, cells from individual plates were trypsinized and counted. (C) Caspase-3 activity levels. Caspase-3 activity was measured in cell extracts, at the time points indicated, using a CPP32/caspase-3 colorimetric protease assay kit (MBL), based on the spectrophotometric detection of the DEVD-pNA cleavage product, pNA. Each reaction well contained 200 μg protein cell extract and 200 μM DEVD-pNA substrate. The results are expressed as a percentage of readings from cell lysates of samples grown in the presence of DMSO, but not subjected to any oligonucleotide treatment. In panels B and C the results are means ± standard errors of six independent determinations.

after 4 days), without reaching baseline levels even 8 days after the transfection (Fig. 2C). These results confirm that apoptotic cell death is amplified by Lon downregulation, and explains why the Z-VAD-FMK addition is able to partially rescue the survival and proliferation of cells during Lon deficiency.

Lon deficiency in human fibroblasts is characterized by low bromodeoxyuridine incorporation and increased generation time

To further investigate the other possible factor causing a lag in cell number, we decided to estimate cell proliferation from the rate of incorporation of bromodeoxyuridine. Although on the second day the cells treated with *lon* antisense oligonucleotide and control oligonucleotide had similar proliferation rates, 6 days after treatment, the *lon* antisense-treated cells were proliferating at a rate 2.5 times slower than the control cells (Table 1). The *lon* antisense oligonucleotide-treated cells were still growing at a reduced rate at a time when the caspase-dependent apotosis was markedly reduced. This slow rate of proliferation may explain why, though not undergoing apoptosis, the Lon-deficient cells still had a slower generation time than the control cells.

Lon proteolytic dysfunction causes accumulation of aggregated proteins in mitochondria

We have previously shown that diminishing Lon levels by treatment with antisense lon oligonucleotides causes the accumulation of both native and carbonylated (oxidized) mitochondrial aconitase as early as the second day after

Table 1
WI-38 VA-13 Lon-depleted cells exhibit diminished proliferation potential, as measured by bromodeoxyuridine (BrdU) incorporation

	Lon antisense oligo. treatment	Control oligo. treatment
Day 2	83.8 ± 3.7%	74.0 ± 9.6%
Day 4	61.0 ± 1.6%	83.1 ± 4.5%
Day 6	51.3 ± 5.7%	124.0 ± 9.8%
Day 8	77.3 ± 3.1%	161.0 ± 11.6%

WI-38 VA-13 human lung fibroblast cells treated with *lon* antisense oligonucleotide or the matched control oligonucleotide were seeded 6 h before each experimental point at a density of 10^4 cells per well into 96 well culture plates. The cells were then incubated with BrdU for 2 h. BrdU incorporation was estimated by enzyme immunoassay (Oncogene), at the time points indicated, and quantified as absorbance (450–550 nm). The results are expressed as percentage of incorporation in untreated cells, where 100% represents BrdU incorporation for cells not subjected to any oligonucleotide treatment.

treatment [24]. Accumulation of oxidized, inactivated aconitase was linked with decrease in aconitase activity both in our system [24] and in aging Drosophila [48] and MnSOD-deficient mice [49]. In the invertebrate system, the inactivation of aconitase has been associated with reduced lifespan. We can now extend these results at a morphological level, by electron microscopy.

Thin-section electron microscopy of control oligonucleotide-treated cells at 20,000× magnification (Fig. 3) revealed mitochondria with the normal profiles of round/ovoid shapes, numerous cristae, and almost transparent matrix (Fig. 3A). In contrast, the mitochondrial matrix of Lon-deficient cells contained electron-dense inclusion bodies, a phenotype previously seen in the *Δpim1* yeast strain [17] and proposed to be caused by aggregated proteins (Fig. 3C). The membranes also had increased electron density probably also due to the accumulation of undegraded or unfolded proteins (Fig. 3C), due to the loss of both the proteolytic and the chaperone activities of the Lon protein. We also identified giant mitochondria in which the matrix space was filled with electron-dense inclusions (Fig. 3C), that structurally resembled the lack of segmentation and the filamentous growth seen in *E. coli* Lon/La mutants [15]. Finally, we observed many empty giant vacuoles, which may be generated by opening of the permeability transition pores of giant mitochondria (Fig. 3D). Some mitochondria had little or no cristae (Fig. 3B), and resembled ρ^0 mitochondria, and *Δpim1* yeast [17], which are also deficient in intact mtDNA due to the loss of Lon's protective function in mtDNA maintenace [6].

Loss of Lon function as a chaperone and/or regulator of mitochondrial gene expression may cause impaired respiration and pyrimidine auxotrophy

Since Lon may function as a chaperone involved in the folding and assembly of respiratory complexes independent of its proteolytic activity, and/or may promote stability and replication of the mitochondrial genome, we predicted that respiratory function would be strongly affected by Lon deficiency.

We measured cell respiration, both in intact cells and in digitonin-permeabilized cells, in the presence of a number of mitochondrial respiratory substrates, 4 days after the oligonucleotide treatment, when Lon levels were virtually undetectable [24]. The respiratory rate of intact cells in growth media was five times lower during Lon deficiency than in normal growth, and was similar to the respiratory impairment reported in *Δpim1* yeast cells [6,17]. We also measured maximal oxygen consumption rates of individual respiratory complexes in digitonin-permeabilized cells. Using glutamate and malate as complex 1 substrates, the oxygen consumption rate was decreased by 70%. At complex 2 (succinate) the decrease was also 70%, while at

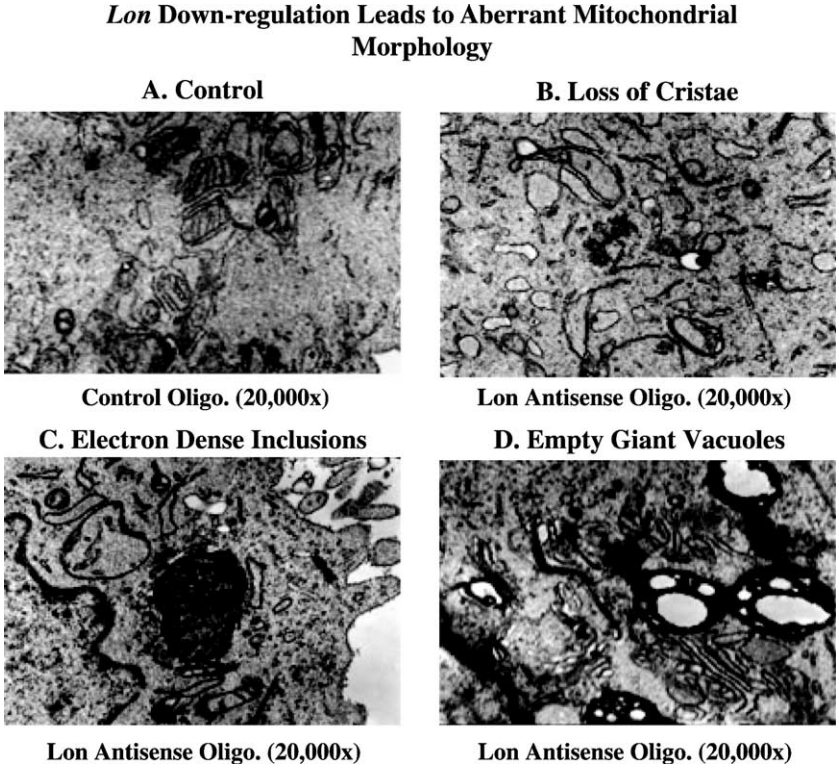

Fig. 3. Mitochondrial defects caused by Lon downregulation. WI-38 VA-13 human lung fibroblasts exposed either to *lon* antisense or to control oligonucleotides were harvested 4 days after the treatment. The cells were prepared by fixing in potassium permanganate, infiltrated with Spurr's resin, sectioned, and contrasted with Reynold's lead citrate. Pictures of mitochondrial defects were taken in many different sections, and the phenotypes described were equally widespread in all the fields studied.

complex 3 (glycerophosphate) and complex 4 (ascorbate and TMPD) respiratory rates were respectively 55 and 53% lower in cells treated with the *lon* antisense oligonucleotides than in control cells (Fig. 4A).

The activity of various other enzymes situated in the mitochondrial inner membrane also requires mitochondrial electron transport for normal function. Among the most important of these is dehydrooratate dehydrogenase, an enzyme in the pyrimidine biosynthetic pathway, that is required for the production of uridine [50]. The need for exogenous uridine addition for cell growth and division is considered a marker for severely dysfunctional mitochondria, and was first associated with (ρ^0) mitochondria lacking mtDNA [33]. Our Lon-deficient cells were also uridine deficient, as evidenced by the fact that we were able to stimulate division of the *lon* antisense-treated cells when we supplemented the growth medium with uridine. After 4 days in the presence of uridine, the growth rate significantly increased (Fig. 4B).

Early loss of mitochondrial transmembrane potential and late decline in mitochondrial mass characterize the lon-deficient phenotype

In order to further investigate the mitochondrial defects leading to low oxygen consumption capacity and a requirement for uridine to sustain cell growth, we next measured mitochondrial transmembrane electrical potential ($\Delta\psi$). At the same time when other mitochondrial markers became altered (Day 4 after the oligonucleotide treatment), we stained cells using MitoLight ($C_{25}H_{27}C_{l3}N_4$) dye [51] (Fig. 5A).

As expected from our study of respiration (Fig. 4), the Lon-deficient cells had decreased transmembrane potential, as shown by the fact that MitoLight accumulated mostly inside the cytoplasm where it was measured predominantly on the green channel. In contrast, in the control oligonucleotide-treated cells, MitoLight was transported inside the active mitochondria, and a significant fraction was visualized on the red channel (Fig. 5B). This result is in agreement with recently published data, showing that Lon overexpression can protect mitochondria from loss of membrane potential following hypoxia and ER stress [31].

We also wanted to determine if the apparent decrease in accumulation of MitoLight inside the *lon* antisense oligonucleotide-treated cells was indeed due to diminished mitochondrial trans-membrane potential, or to a decline in the total number of mitochondria inside these cells. When we used a mitochondrial dye, Mito Fluor Red 589, which accumulates inside mitochondrial membrane lipids, regardless of membrane potential, we were not able to detect any difference in the total mass of mitochondrial membranes between the two experimental groups by FACS analysis 4 days after treatment (Fig. 6). Two days later however, on Day 6, a population of cells with less mitochondria began to appear in the cells with decreased Lon content (indicated by the arrow in the bottom right panel of Fig. 5). This observation validates the hypothesis that Lon is involved in mitochondrial biogenesis [30], and may explain the similarity but lack of complementation between the *Δpim1* and the ρ^0 strains in yeast [6,17].

The combined results of Figs. 5 and 6 provide good evidence for an early loss of mitochondrial transmembrane potential, followed by a subsequent decrease in overall mitochondrial mass, during Lon antisense-induced Lon deficiency.

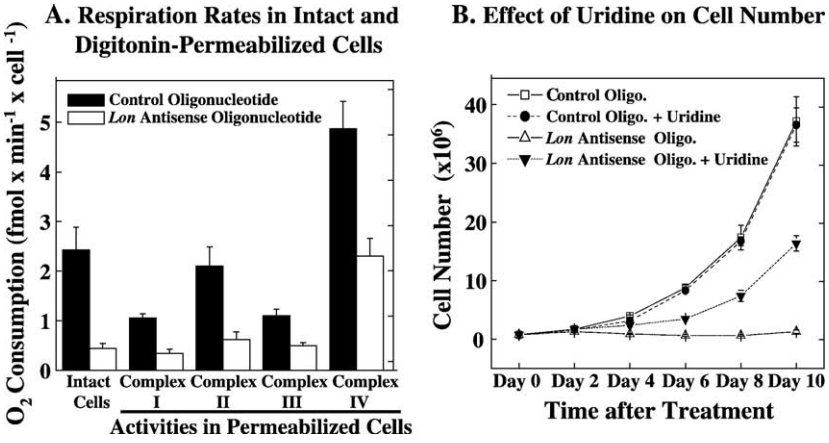

Fig. 4. Lower respiratory rates and uridine auxotrophy after *lon* antisense oligonucleotide treatment. (A) Lon deficiency causes reduced cellular and mitochondrial respiratory rates. WI-38 VA-13 human lung fibroblasts were treated with *lon* antisense oligonucleotide, or the matched control oligonucleotide. Four days after treatment, the cells were harvested, and respiratory rates were calculated for the intact cells as well as for digitonin-permeabilized cells using 5×10^6 cells in each assay. Substrates used included glutamate + malate (complex I), succinate (complex II), glycerol 3-phosphate (complex III), and ascorbate + TMPD (complex IV) substrates. Oxygen consumption was measured using a Rank Brothers, Clark-type electrode in 1.5 ml medium, as described under Experimental procedures. (B) WI-38 VA-13 Lon-depleted cells display pyrimidine auxotrophy. WI-38 VA-13 cells were grown after the oligomorpholine treatment in the absence or presence of uridine (100 μg/ml). At the time points indicated, cells from individual plates were trypsinized and counted. In both panels A and B all data points shown are the means ± standard errors of six independent determinations.

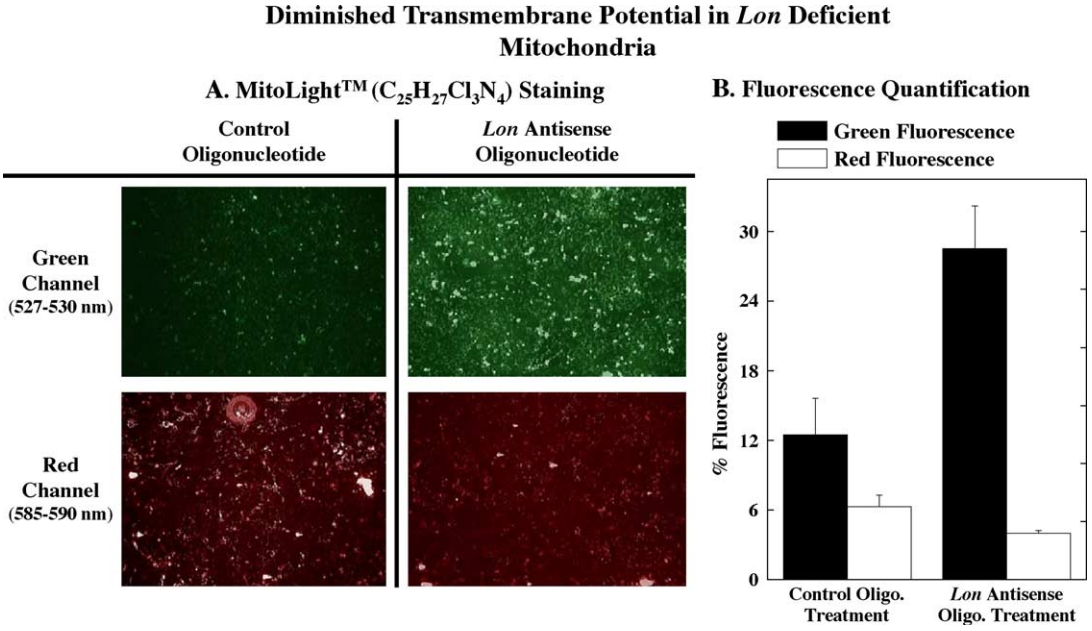

Fig. 5. Decreased mitochondrial transmembrane potential in *lon* antisense oligonucleotide-treated WI-38 VA-13 cells, measured by fluorescence microscopy. (A) WI-38 VA-13 human lung fibroblast cells were treated with antisense *lon* oligonucleotide, or the matched control oligonucleotide. Four days after treatment, adherent cells were stained with MitoLightTM ($C_{25}H_{27}C_{l3}N_4$) from Chemicon. (B) Summary of means and standard errors of green (527–530 nm) and red (585–590 nm) channel fluorescence from three individual experiments, quantified by densitometry (IP Lab) and expressed in arbitrary fluorescence units.

Respiration-impaired, Lon-deficient cells rely on anaerobic energy metabolism

The Lon-deficient cells needed frequent media changes to maintain pH, and to replenish glucose/pyruvate stores. During all our experiments involving Lon-deficient cells, daily changes of Eagle's minimum essential medium were required in order to maintain the cells attached to the culture plates. Furthermore, the 1-day-old media were already acidic, as shown by the color change of the pH marker, Phenol Red, from pink to light yellow. These, and other observations show that the Lon-deficient cells were largely dependent on anaerobic energy metabolism.

Cell death estimation as a function of actual cell number and proliferation rates

We have calculated the percentage of cells that died at intervals of 2 days, by estimating the predicted number of cells at the end of each interval, based on the growth rates

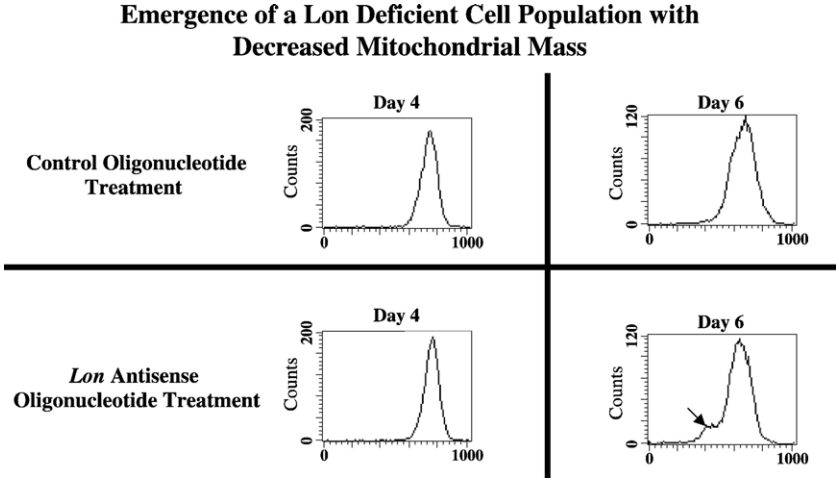

Fig. 6. Decreased mitochondrial mass in *lon* antisense oligonucleotide-treated WI-38 VA-13 cells, measured by FACS analysis. WI-38 VA-13 human lung fibroblast cells were treated with antisense *lon* oligonucleotide, or the matched control oligonucleotide. Four and 6 days after treatment, the cells were trypsinized and stained with Mito Fluor Red 589 (Molecular Probes), which accumulates in mitochondrial membrane lipids (regardless of membrane potential). FACS analysis was performed at 588 nm (emission) and 622 nm (excitation), as recommended by the manufacturer. The data shown are representative of several experiments.

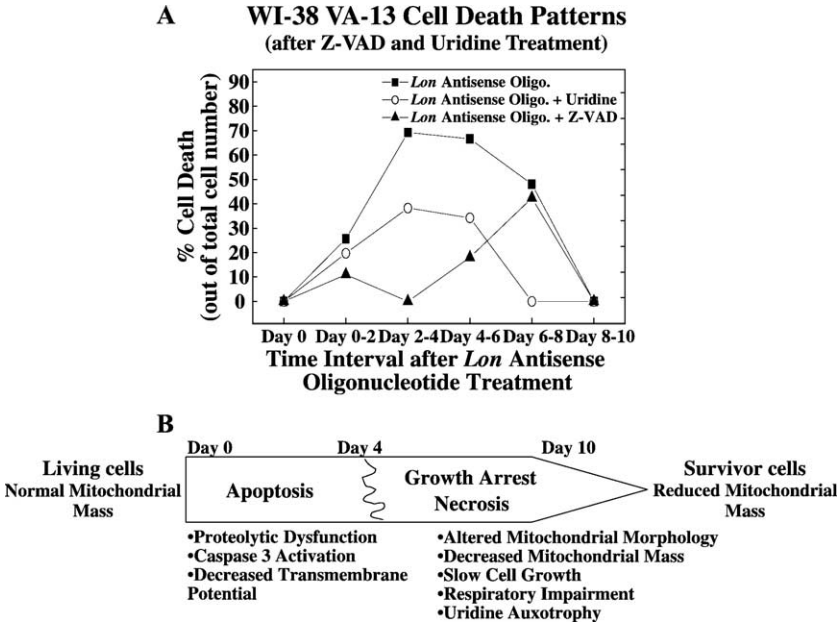

Fig. 7. Lon-deficient cell death patterns after Z-VAD and uridine treatment. (A) *Lon* antisense oligonucleotide-treated cells were counted every second day after the transfection treatment. At the same points in time, the rate of cell growth estimated by BrdU incorporation was measured. The number of cells that died was calculated as the difference between the predicted cell number and the actual cell number, divided by growth rate. (B) Schematic representation of stages of Lon deficiency in WI-38 VA-13 fibroblasts from apoptosis to selection of survivor cells with reduced mitochondrial mass.

calculated from bromodeoxyuridine incorporation. The difference between the predicted number of cells and the actual number measured was considered to represent the predicted progenies of cells that died, and this difference was divided by the growth rate, in order to calculate the actual number of cells that died instead of dividing (Fig. 7A).

Using this algorithm, we were able to calculate that, during Lon protease deficiency, an increased number of cells died between Day 2 and Day 6, and then the cell death rate declined, reaching baseline after 8 days. The two agents that we used to compensate for Lon deficiency acted at different stages of Lon-induced lethality. Z-VAD-FMK was able to reduce cell death almost completely in the first 4 days but it became less efficient after Day 4, and exerted no effect at all by Day 6. In contrast, uridine addition had only a small effect during the initial phase of massive apoptosis, but effectively reduced cell death by 50% at Day 4, and even reestablished normal cell growth and division by Day 6. This temporal pattern probably argues for two types of cell death induced by loss of Lon function: an initial apoptosis followed by mitochondrial dysfunction, ATP deficiency and eventual necrosis, and final selection of survivor cells with diminished mitochondrial content (Fig. 7B).

Discussion

Very little information is available about the function of the Lon protease in higher organisms, especially humans. In this paper, we analyze the first human cell model of Lon deficiency, obtained by downregulating Lon expression in WI-38 VA-13 human lung fibroblasts [24]. Since the *E. coli* protease La and the yeast Lon protease have been more extensively studied, we also compared our results with previously published observations on these two organisms.

Lon downregulation in WI-38 VA-13 human lung fibroblasts elicits two temporally and mechanistically distinctive patterns. Initially, loss of Lon activity causes massive apoptosis, with the classic hallmark of caspase-3 activation. At this early stage we can also partially improve cell survival by addition of the caspase-3 inhibitor, Z-VAD-FMK. Two Lon functions seem to be mostly involved in this early apoptosis: the proteolytic defect causes accumulation of aggregated proteins inside mitochondria; while loss of chaperone function severely affects mitochondrial respiration and membrane potential, rendering cells extremely susceptible to apoptotic stimuli. At a later stage, the surviving cells lose their ability to undergo apoptosis, and are respiratory deficient and unable to divide due to defects in uridine synthesis. Lon involvement in mitochondrial division and maintenance of mitochondrial mass also becomes apparent, as a population of cells with diminished mitochondrial content emerges.

Inhibitors of respiratory complexes, such as rotenone [52] and antimycin [53], have previously been shown to be able to cause apoptosis, and the availability of intracellular ATP plays a major role in cell survival or the type of cell death [54,55]. The demise of cells after an apoptotic trigger has been shown to be a continuum governed by the intracellular ATP concentration: cells with adequate energy supplies undergo apoptosis, while cells with progressive ATP depletion switch to cell death with mixed features (apoptonecrosis), and then, finally to necrosis [53,56]. We propose that the type of cell death in the Lon-deficient cells is also

controlled by the level of ATP depletion caused by severe mitochondrial defects at both a functional (loss of aerobic respiration and membrane potential) and a morphological level, involving accumulation of aggregated, oxidatively damaged proteins, such as aconitase [24], or unassembled respiratory chain subunits [23,31]. Thus, while apoptosis predominates in the early days after transfection, energy production is subsequently compromised and the cells enter growth arrest and necrosis. It is entirely possible that the cell death pattern observed between Days 4 and 8 of *lon* antisense treatment may actually conform to the mitoptosis pathway proposed by Skulachev [57,58]. The fact that *lon* downregulation can induce apoptosis or render cells more sensitive to apoptotic stimuli is especially important since in other systems where decreased Lon levels have been described, i.e., aging [29] and *Sod2*$^{-/+}$ murine muscle [59], increased rates of apoptotic cell death [60,61] have also been reported.

Most of the mitochondrial dysfunctions described in this paper seem to be caused by a combination of the three functions of Lon described in eukaryotes, and in addition, mimic some of the *lon/la* knockout phenotypes in *E. coli*, though no similar mechanisms have yet been described in mitochondria. The major decrease in oxygen consumption capacity produced by Lon downregulation can be explained by Lon's dual function as a protease and as a chaperone [23]. Lon removes damaged enzymes, such as oxidized aconitase, from the matrix [24]. Lon also assists with the folding and assembly of the matrix and inner membrane respiratory chain complexes [23,31] during their processing inside the mitochondrial matrix, following synthesis (for the mitochondrially encoded subunits), or after import into mitochondria (for the nuclear encoded subunits).

Changes in mitochondrial morphology argue for a rather complex and heterogenous mechanism, probably also dependent on the levels of Lon required for a specific function in each distinctive mitochondrial population. The presence of electron-dense inclusion bodies inside mitochondria, which are presumably formed from aggregated proteins, confirms our previous observations that oxidized aconitase (and other damaged proteins) accumulate during Lon proteolytic deficiency [24]. Mitochondria with little or no cristae (ρ^0-like mitochondria) seen by electron microscopy, and the emergence of a cell subpopulation with decreased mitochondrial content, are more evidence of Lon's function in maintaining mtDNA integrity and stimulating mitochondrial biogenesis. While no homolog of the DNA damage-induced SulA, which acts as a cell division inhibitor after ultraviolet light damage [13], has been described in mitochondria, the appearance of giant mitochondrial bodies inside the cytoplasm of Lon-deficient WI-38 VA-13 fibroblasts suggests that the lack of septation and filamentous growth [15] which characterize the *ΔLon/La E. coli* strains might be also taking place in these cell's mitochondria.

In conclusion, Lon protease emerges as a major controller of multiple human mitochondrial functions, including the assembly of respiratory chain protein complexes, the degradation of (oxidatively) damaged proteins, and the maintenance of mitochondrial DNA integrity. However, although the protease is highly conserved [17,27,28], some of its functions might not be the same, or be performed in the same manner, in different organisms. In *E. coli*, protease Lon/La is involved in a number of adaptative processes, either by selective degradation of short-lived regulatory proteins such as UmuD and UmuC of the SOS response [12] or by generalized degradation of free ribosomal proteins [16]. Only a few specific substrates of Lon protease have been identified in mammalian systems [24], and none of them should be involved in mitochondrial DNA maintenance. However, Lon homeostasis is crucial to mammalian cell fate, as *lon* upregulation is associated with tumorigenic transformation [62] and *lon* downregulation leads to apoptosis. Thus, further studies in animal systems are needed to explain the specific pathways controlled by Lon, and to develop an advanced understanding of Lon involvement in apoptosis and carcinogenesis.

Acknowledgment

This research was partially supported by NIH/NIEHS grant #ES 03598 to K.J.A.D.

References

[1] Gottesman, S. Proteases and their targets in Escherichia coli. *Annu. Rev. Genet.* **30:**465–506; 1996.
[2] Chin, D. T.; Goff, S. A.; Webster, T.; Smith, T.; Goldberg, A. L. Sequence of the lon gene in Escherichia coli: a heat-shock gene which encodes the ATP-dependent protease La. *J. Biol. Chem.* **263:** 11718–11728; 1988.
[3] Ito, K.; Udaka, S.; Yamagata, H. Cloning, characterization, and inactivation of the Bacillus brevis lon gene. *J. Bacteriol.* **174:** 2281–2287; 1992.
[4] Gill, R. E.; Karlok, M.; Benton, D. Myxococcus xanthus encodes an ATP-dependent protease which is required for developmental gene transcription and intercellular signaling. *J. Bacteriol.* **175:**4538–4544; 1993.
[5] Tojo, N.; Inouye, S.; Komano, T. Cloning and nucleotide sequence of the Myxococcus xanthus lon gene: indispensability of lon for vegetative growth. *J. Bacteriol.* **175:**2271–2277; 1993.
[6] Van Dyck, L.; Pearce, D. A.; Sherman, F. PIM1 encodes a mitochondrial ATP-dependent protease that is required for mitochondrial function in the yeast Saccharomyces cerevisiae. *J. Biol. Chem.* **269:**238–242; 1994.
[7] Desautels, M.; Goldberg, A. L. Demonstration of an ATP-dependent, vanadate-sensitive endoprotease in the matrix of rat liver mitochondria. *J. Biol. Chem.* **257:**11673–11679; 1982.
[8] Watabe, S.; Kimura, T. ATP-dependent protease in bovine adrenal cortex. Tissue specificity, subcellular localization, and partial characterization. *J. Biol. Chem.* **260:**5511–5517; 1985.
[9] Watabe, S.; Kimura, T. Adrenal cortex mitochondrial enzyme with ATP-dependent protease and protein-dependent ATPase activities: purification and properties. *J. Biol. Chem.* **260:**14498–14504; 1985.
[10] Chung, C. H.; Goldberg, A. L. The product of the lon (capR) gene in

Escherichia coli is the ATP-dependent protease, protease La. *Proc. Natl. Acad. Sci. USA* **78:**4931–4935; 1981.
[11] Goldberg, A. L.; Moerschell, R. P.; Chung, C. H.; Maurizi, M. R. ATP-dependent protease La (lon) from Escherichia coli. *Method Enzymol.* **244:**350–375; 1994.
[12] Frank, E. G.; Ennis, D. G.; Gonzalez, M.; Levine, A. S.; Woodgate, R. Regulation of SOS mutagenesis by proteolysis. *Proc. Natl. Acad. Sci. USA* **93:**10291–10296; 1996.
[13] Mizusawa, S.; Gottesman, S. Protein degradation in Escherichia coli: the lon gene controls the stability of sulA protein. *Proc. Natl. Acad. Sci. USA* **80:**358–362; 1983.
[14] Torres-Cabassa, A. S.; Gottesman, S. Capsule synthesis in Escherichia coli K-12 is regulated by proteolysis. *J. Bacteriol.* **169:**981–989; 1987.
[15] Schoemaker, J. M.; Gayda, R. C.; Markovitz, A. Regulation of cell division in Escherichia coli: SOS induction and cellular location of the sulA protein, a key to lon-associated filamentation and death. *J. Bacteriol.* **158:**551–561; 1984.
[16] Kuroda, A.; et al. Role of inorganic polyphosphate in promoting ribosomal protein degradation by the Lon protease in E. coli. [see comments.]. *Science* **293:**705–708; 2001.
[17] Suzuki, C. K.; Suda, K.; Wang, N.; Schatz, G. Requirement for the yeast gene LON in intramitochondrial proteolysis and maintenance of respiration [erratum appears in Science 1994 May 13;264(5161):891]. *Science* **264:**273–276; 1994.
[18] van Dyck, L.; Neupert, W.; Langer, T. The ATP-dependent PIM1 protease is required for the expression of intron-containing genes in mitochondria. *Genes Dev.* **12:**1515–1524; 1998.
[19] Van Dyck, L.; Langer, T. ATP-dependent proteases controlling mitochondrial function in the yeast Saccharomyces cerevisiae. *Cell. Molec. Life Sci.* **56:**825–842; 1999.
[20] Teichmann, U.; et al. Substitution of PIM1 protease in mitochondria by Escherichia coli Lon protease. *J. Biol. Chem.* **271:**10137–10142; 1996.
[21] Fu, G. K.; Markovitz, D. M. The human LON protease binds to mitochondrial promoters in a single-stranded, site-specific, strand-specific manner. *Biochemistry* **37:**1905–1909; 1998.
[22] Langer, T.; Neupert, W. Regulated protein degradation in mitochondria. *Experientia* **52:**1069–1076; 1996.
[23] Rep, M.; et al. Promotion of mitochondrial membrane complex assembly by a proteolytically inactive yeast Lon [erratum appears in Science 1997 Feb 7;275(5301):741.]. *Science* **274:**103–106; 1996.
[24] Bota, D. A.; Davies, K. J. A. Lon protease preferentially degrades oxidized mitochondrial aconitase by an ATP-stimulated mechanism. *Nature Cell Biol.* **4:**674–680; 2002.
[25] Watabe, S.; et al. Purification and characterization of a substrate protein for mitochondrial ATP-dependent protease in bovine adrenal cortex. *J. Biochem.* **115:**648–654; 1994.
[26] Liu, T.; et al. DNA and RNA binding by the mitochondrial lon protease is regulated by nucleotide and protein substrate. *J. Biol. Chem.* **279:**13902–13910; 2004.
[27] Amerik, A., et al. Cloning and sequence analysis of cDNA for a human homolog of eubacterial ATP-dependent Lon proteases. *FEBS Lett.* **340:**25–28; 1994.
[28] Wang, N.; Gottesman, S.; Willingham, M. C.; Gottesman, M. M.; Maurizi, M. R. A human mitochondrial ATP-dependent protease that is highly homologous to bacterial Lon protease. *Proc. Natl. Acad. Sci. USA* **90:**11247–11251; 1993.
[29] Lee, C. K.; Klopp, R. G.; Weindruch, R.; Prolla, T. A. Gene expression profile of aging and its retardation by caloric restriction [see comments]. *Science* **285:**1390–1393; 1999.
[30] Luciakova, K.; Sokolikova, B.; Chloupkova, M.; Nelson, B. D. Enhanced mitochondrial biogenesis is associated with increased expression of the mitochondrial ATP-dependent Lon protease. *FEBS Lett.* **444:**186–188; 1999.
[31] Hori, O.; et al. Transmission of cell stress from endoplasmic reticulum to mitochondria: enhanced expression of Lon protease. *J. Cell Biol.* **157:**1151–1160; 2002.
[32] Summerton, J. Morpholino antisense oligomers: design, preparation, and properties. *Antisense Nucleic Acid Drug Dev.* **7:**187–195; 1997.
[33] King, M. P.; Attardi, G. Isolation of human cell lines lacking mitochondrial DNA. *Methods Enzymol.* **264:**304–313; 1996.
[34] Fiskum, G.; Craig, S. W.; Decker, G. L.; Lehninger, A. L. The cytoskeleton of digitonin-treated rat hepatocytes. *Proc. Natl. Acad. Sci. USA* **77:**3430–3434; 1980.
[35] Hofhaus, G.; Shakeley, R. M.; Attardi, G. Use of polarography to detect respiration defects in cell cultures. *Methods Enzymol.* **264:**476–483; 1996.
[36] Schoonen, W. G.; Wanamarta, A. H.; van der Klei-van Moorsel, J. M.; Jakobs, C.; Joenje, H. Respiratory failure and stimulation of glycolysis in Chinese hamster ovary cells exposed to normobaric hyperoxia. *J. Biol. Chem.* **265:**1118–1124; 1990.
[37] Godbey, W. T.; Wu, K. K.; Mikos, A. G. Poly(ethylenimine)-mediated gene delivery affects endothelial cell function and viability. *Biomaterials* **22:**471–480; 2001.
[38] Colombaioni, L.; Colombini, L.; Garcia-Gil, M. Role of mitochondria in serum withdrawal-induced apoptosis of immortalized neuronal precursors. *Brain Res. Dev. Brain Res.* **134:**93–102; 2002.
[39] Galli, G.; Fratelli, M. Activation of apoptosis by serum deprivation in a teratocarcinoma cell line: inhibition by L-acetylcarnitine. *Exp. Cell Res.* **204:**54–60; 1993.
[40] Gu, J.; et al. Evidence that increased 12-lipoxygenase activity induces apoptosis in fibroblasts. *J. Cell. Physiol.* **186:**357–365; 2001.
[41] Walker, P. R.; et al. Topoisomerase II-reactive chemotherapeutic drugs induce apoptosis in thymocytes. *Cancer Res.* **51:**1078–1085; 1991.
[42] Darzynkiewicz, Z.; et al. Features of apoptotic cells measured by flow cytometry. *Cytometry* **13:**795–808; 1992.
[43] Nicoletti, I.; Migliorati, G.; Pagliacci, M. C.; Grignani, F.; Riccardi, C. A rapid and simple method for measuring thymocyte apoptosis by propidium iodide staining and flow cytometry. *J. Immunol. Methods* **139:**271–279; 1991.
[44] Pagliacci, M. C.; Tognellini, R.; Grignani, F.; Nicoletti, I. Inhibition of human breast cancer cell (MCF-7) growth in vitro by the somatostatin analog SMS 201-995: effects on cell cycle parameters and apoptotic cell death. *Endocrinology* **129:**2555–2562; 1991.
[45] Nicholson, D. W.; et al. Identification and inhibition of the ICE/CED-3 protease necessary for mammalian apoptosis [see comments.]. *Nature* **376:**37–43; 1995.
[46] Patel, T.; Gores, G. J.; Kaufmann, S. H. The role of proteases during apoptosis. *FASEB J.* **10:**587–597; 1996.
[47] Fujii, Y.; et al. Mitochondrial cytochrome c release and caspase-3-like protease activation during indomethacin-induced apoptosis in rat gastric mucosal cells. *Proc. Soc. Exp. Biol. Med.* **224:**102–108; 2000.
[48] Yan, L. J.; Levine, R. L.; Sohal, R. S. Oxidative damage during aging targets mitochondrial aconitase [erratum appears in Proc. Natl. Acad. Sci. USA 1998 Feb 17;95(4):1968]. *Proc. Natl. Acad. Sci. USA* **94:**11168–11172; 1997.
[49] Williams, M. D., et al. Increased oxidative damage is correlated to altered mitochondrial function in heterozygous manganese superoxide dismutase knockout mice. *J. Biol. Chem.* **273:**28510–28515; 1998.
[50] Gregoire, M.; Morais, R.; Quilliam, M. A.; Gravel, D. On auxotrophy for pyrimidines of respiration-deficient chick embryo cells. *Eur. J. Biochem.* **142:**49–55; 1984.
[51] Smiley, S. T.; et al. Intracellular heterogeneity in mitochondrial membrane potentials revealed by a J-aggregate-forming lipophilic cation JC-1. *Proc. Natl. Acad. Sci. USA* **88:**3671–3675; 1991.
[52] Armstrong, J. S.; Hornung, B.; Lecane, P.; Jones, D. P.; Knox, S. J. Rotenone-induced G2/M cell cycle arrest and apoptosis in a human B lymphoma cell line PW. *Biochem. Biophys. Res. Commun.* **289:** 973–978; 2001.
[53] Formigli, L.; et al. Aponecrosis: morphological and biochemical exploration of a syncretic process of cell death sharing apoptosis and necrosis. *J. Cell. Physiol.* **182:**41–49; 2000.
[54] Eguchi, Y.; Shimizu, S.; Tsujimoto, Y. Intracellular ATP levels

determine cell death fate by apoptosis or necrosis. *Cancer Res.* **57:**1835–1840; 1997.

[55] Leist, M.; Single, B.; Castoldi, A. F.; Kuhnle, S.; Nicotera, P. Intracellular adenosine triphosphate (ATP) concentration: a switch in the decision between apoptosis and necrosis. *J. Exp. Med.* **185:** 1481–1486; 1997.

[56] Formigli, L.; Zecchi Orlandini, S.; Capaccioli, S.; Poupon, M. F.; Bani, D. Energy-dependent types of cell death in MCF-7 breast cancer cell tumors implanted into nude mice. *Cells Tissues Organs* **170:**99–110; 2002.

[57] Skulachev, V. P. The programmed death phenomena, aging, and the Samurai law of biology. *Exp. Gerontol.* **36:**995–1024; 2001.

[58] Skulachev, V. P. Programmed death phenomena: from organelle to organism. *Ann. N.Y. Acad.Sci.* **959:**214–237; 2002.

[59] Bota, D. A.; Van Remmen, H.; Davies, K. J. Modulation of Lon protease activity and aconitase turnover during aging and oxidative stress. *FEBS Lett.* **532:**103–106; 2002.

[60] Dirks, A.; Leeuwenburgh, C. Apoptosis in skeletal muscle with aging. *Am. J. Physiol. - Regul. Integr. Comp. Physiol.* **282:**R519–R527; 2002.

[61] Van Remmen, H.; et al. Knockout mice heterozygous for Sod2 show alterations in cardiac mitochondrial function and apoptosis. *Am. J. Physiol.* **281:**H1422–H1432; 2001.

[62] Zhu, Y.; et al. Epidermal growth factor up-regulates the transcription of mouse lon homology atp-dependent protease through extracellular signal-regulated protein kinase- and phosphatidylinositol-3-kinase-dependent pathways. *Exp. Cell Res.* **280:**97–106; 2002.